

Development of Predictive Current Controller for Multi-Port DC/DC Converter

Santhosh T K and Govindaraju C

Department of Electrical and Electronics Engineering, Government College of Engineering, Salem, India

Article Info

Article history:

Received Jul 03, 2015

Revised Aug 14, 2015

Accepted Aug 29, 2015

Keyword:

Multiple Input Converter
Predictive Current Control
Hybrid Electric Vehicle
Ultracapacitor
Digital Signal Processor

Corresponding Author:

T.K. Santhosh
Department of Electrical and Electronics Engineering
Government College of Engineering, Salem, India
Email: tksanthosh.kct@gmail.com

ABSTRACT

This paper investigates the utilization of a predictive current control for a four port DC/DC power electronic converter with an input port, two storage ports and a load port suitable for a Hybrid Electric Vehicle. Being a power converter with multiple ports, it has different operating modes. While the Stateflow controller is employed to handle mode selection, the predictive current controller is used to control the inductor current. The control laws governing each operating mode is derived out for valley current control. By making the inductor current in the upcoming switching cycle equivalent to the reference, the duty cycle is predicted. Simulation and experimental results show improvements in current ripple minimization, faster dynamic performance and comparable to traditional PI control method.

Copyright © 2015 Institute of Advanced Engineering and Science.
All rights reserved.

1. INTRODUCTION

The recent developments in the power processing and storage technology are promoting electric propulsion. Different power converter topologies suitable for automotive applications have found renewed interest in the recent past. During the course of its evolution, many sources and storage units have found its place in a Hybrid Electric Vehicle. Different topologies incorporating multiple input and output ports have been developed in the past. These power converters employ different control techniques to achieve control objectives [1]. The control objective could be target current [2, 3] or voltage [4], the limit on a ripple [5], faster or slower response [6] and quick recovery from a disturbance or a stability criterion [7]. Traditional control techniques in both analog and digital domain have been in use for an extended period. With the advent of digital control, the traditional analog have transformed into the digital domain, and new controllers are being introduced to control a specific or set of system parameters. Inductor current control is one of the control method that helps to extract constant power from input sources. Inductor current control is usually done by making the inductor current to follow a particular reference to minimize error. The idea of predictive control is to predict the duty cycle of the succeeding switching cycles based on the measured system parameters. The predictive current could be of three types: valley, peak or average current. Out of these three, valley current control is investigated in this work for trailing edge modulation. The Predictive Current Control (PCC) is applied to a Four Port Converter proposed in [8]. Control laws are derived for each operating mode, and the performance is analyzed both through simulation and experimental results.

The concept of predictive control [9, 10, 11, 12] is to predict the duty cycle command for the upcoming switching periods based on the present and past status of system parameters. The topology selected in this work necessitates a strict constraint on the inductor current that shall be fulfilled by the predictive current control technique. Each mode necessitates a separate control law. However, from the analysis, it has been found that the first four operating modes utilize a similar control law with different parameters for duty cycle computation. So the same control law could be implemented for the modes I-IV, by switching the parameters used for computation. Mode V and VI utilize a separate control law for duty cycle command computation. By making the predicted current equal to the

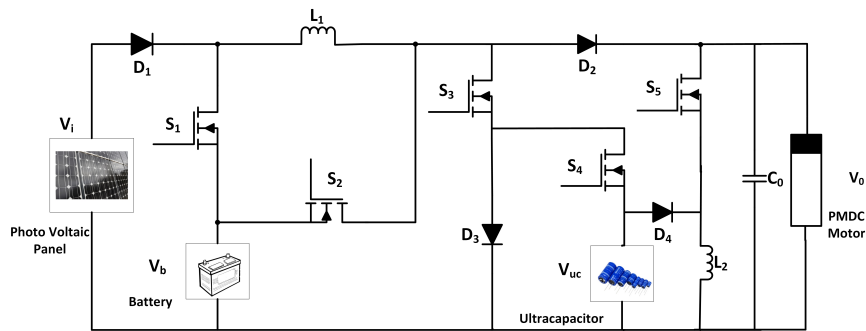


Figure 1. Four Port Converter for Hybrid Electric Vehicle

reference current in the computation of duty cycle, the reference current could be easily achieved. The originality of the work lies in the utilization of predictive controller for the inductor current inductor current and its implementation to the Four Port Converter.

The rest of the paper is organized as follows: section II presents the details of the power converter topology, section III deals with different operating modes and the derivation of control laws, section IV explains the control law implementation, section V presents the results and section VI concludes the paper.

2. TOPOLOGY

A Four Port Converter with an input port (V_i), two storage ports (V_b , V_{uc}) and a load port (V_0) suitable for Hybrid Electric Vehicle applications is considered for the implementation of predictive current control. The power circuit of the converter is shown in Figure 1. Being a multi-port topology, it has six different operating modes. Each operating mode has two different switching states. A summary of all the operating modes with the first switching state denoted by the darkened lines and the second switching state represented by discontinuous red line is shown in Figure 2 and Figure 3. The detailed synthesis and analysis of the four port converter is handled in [8]. This converter requires two different controllers: one for mode selection and other for inductor current regulation. A Stateflow controller is used for mode selection and the predictive control is used for current regulation. The Predictive Current Controller has to respond to sudden variations in modes and system parameters. Our investigation is limited to the utilization of predictive current control for inductor current regulation.

3. PREDICTIVE CURRENT CONTROL FOR FPC

This section presents the control law derivation for each operating mode. To begin with, the inductor current waveform is considered and a duty cycle is derived using the charge-second balance. The duty cycle calculation is then extended to the another switching period to find the final expression.

3.1. Mode I

In the first operating mode (refer Figure 2(a)), energy is transferred from the primary source port (V_i) to the load (V_0). In the first state (denoted by darkened lines) S_3 , D_1 , and D_3 are ON and during the second switching state (denoted by discontinuous red line), switching devices D_1 and D_2 are turned ON. The charging slope is given by V_i/L_1 and the discharging slope is given by $(V_i - V_0)/L_1$ as shown in Figure 4. Assuming the converter operates in Continuous Conduction Mode (CCM), the next switching cycle also repeats the same behavior. The inductor current $i(n)$ in n^{th} switching cycle is given by,

$$i(n) = i(n-1) + \frac{V_i d_3 [n] T_s}{L_1} + \frac{(V_i - V_0) d'_3 [n] T_s}{L_1} \quad (1)$$

Where T_s is the switching period and d_3 is the duty cycle of switch S_3 . Extending the same argument to the $(n+1)^{th}$ switching cycle,

$$i(n+1) = i(n-1) + \frac{V_i d_3 [n] T_s}{L_1} + \frac{(V_i - V_0) d'_3 [n] T_s}{L_1} + \frac{V_i d_3 [n+1] T_s}{L_1} + \frac{(V_i - V_0) d'_3 [n+1] T_s}{L_1} \quad (2)$$

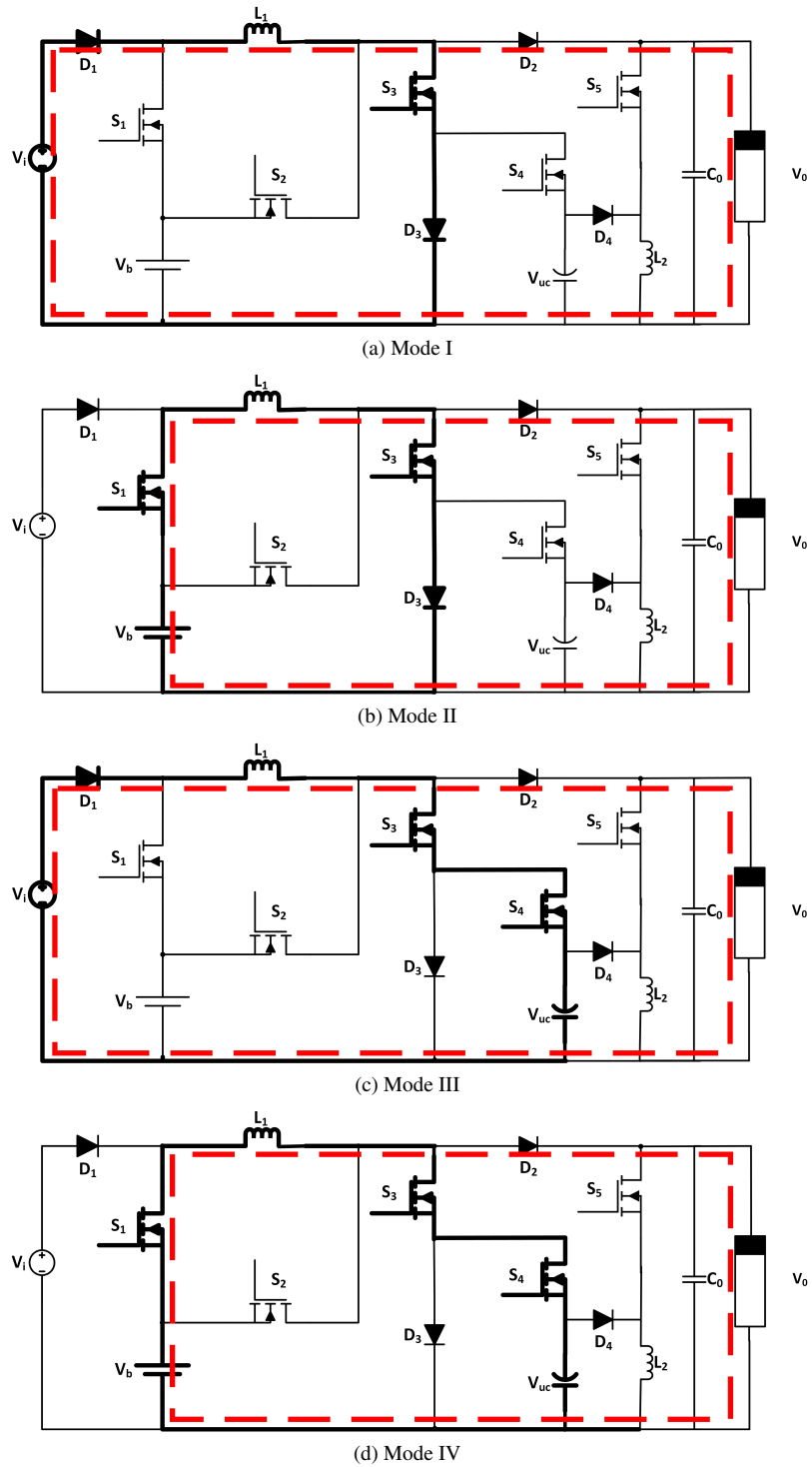


Figure 2. Switching States in Operating Modes I-IV

Grouping variables,

$$i(n + 1) = i(n - 1) + 2 \frac{V_i T_s}{L_1} - \frac{V_0 T_s (d'_3[n] + d'_3[n + 1])}{L_1} \tag{3}$$

Using the relation $d + d' = 1$ and rearranging, the duty cycle for $(n + 1)^{th}$ is given by

$$d_3[n + 1] = 2 - d_3[n] + \frac{L_1}{V_0 T_s} [i(n + 1) - i(n - 1)] - 2 \frac{V_i}{V_0} \tag{4}$$

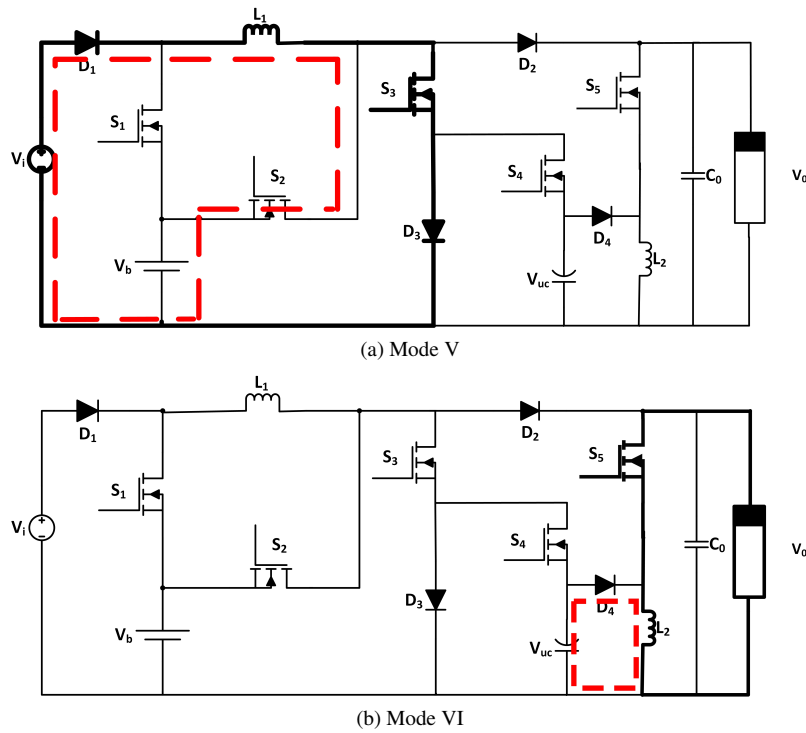


Figure 3. Switching states in Operating Modes V-VI

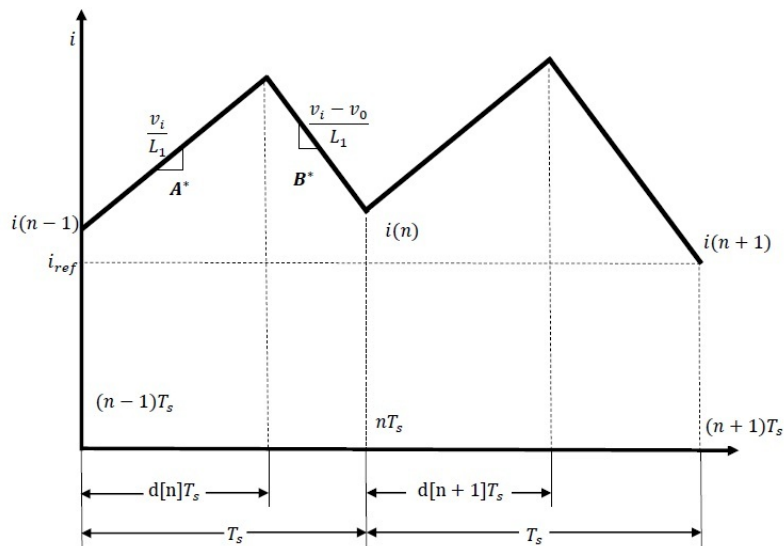


Figure 4. Inductor Current Waveform

3.2. Mode II

In this mode, energy is transferred from the primary storage device (V_b) to the load (refer Figure 2(b)). This mode is initialized when V_i drops below a prefixed threshold level. So the diode D_1 will block the primary source (V_i). In the first state, the switching devices S_1, S_3 and D_3 are turned ON and the switching devices S_1, D_2 are turned ON

during the second switching state. The charging and discharging slope could be found in Table 1. Inductor current for $(n + 1)^{th}$ switching cycle in Mode II is given by,

$$i(n + 1) = i(n - 1) + \frac{V_b d_3[n] T_s}{L_1} + \frac{(V_b - V_0) d'_3[n] T_s}{L_1} + \frac{V_b d_3[n + 1] T_s}{L_1} + \frac{(V_b - V_0) d'_3[n + 1] T_s}{L_1} \quad (5)$$

Simplifying for duty cycle in $(n + 1)^{th}$ switching period,

$$d_3[n + 1] = 2 - d_3[n] + \frac{L_1 [i(n + 1) - i(n - 1)]}{V_0 T_s} - \frac{2V_b}{V_0} \quad (6)$$

Mode	Source Port	Load Port	Description	Charging slope	Discharging slope
I	V_i	V_0	Input source supplying load	$\frac{V_i}{L_1}$	$\frac{V_i - V_0}{L_1}$
II	V_b	V_0	Primary storage supplying load	$\frac{V_b}{L_1}$	$\frac{V_b - V_0}{L_1}$
III	V_i, V_{uc}	V_0	Secondary storage aids Input source to supply load	$\frac{V_i + V_{uc}}{L_1}$	$\frac{V_i - V_0}{L_1}$
IV	V_b, V_{uc}	V_0	Secondary storage aids primary storage to supply load	$\frac{V_b + V_{uc}}{L_1}$	$\frac{V_b - V_0}{L_1}$
V	V_i	V_b	Input source supplying primary storage	$\frac{V_i}{L_1}$	$\frac{V_i - V_b}{L_1}$
VI	V_0	V_{uc}	Regeneration	$\frac{V_0}{L_2}$	$\frac{V_{uc}}{L_2}$

Table 1. Summary of Different Operating Modes

3.3. Mode III

This is a hybrid mode which utilizes power from the primary source (V_i) and secondary storage port (V_{uc}) to the load. This mode (Figure 2(c)) is initialized when the voltage level of the primary source falls below a threshold value. The polarity of the secondary storage is reversed to ensure voltage addition. switching devices S_3, S_4 and D_1 are turned on in state I and during switching state II D_1 and D_2 are ON. The inductor current in $(n + 1)^{th}$ cycle is given by,

$$i(n + 1) = i(n - 1) + \frac{(V_i + V_{uc}) d_4[n] T_s}{L_1} + \frac{(V_i - V_0) d'_4[n] T_s}{L_1} + \frac{(V_i + V_{uc}) d_4[n + 1] T_s}{L_1} + \frac{(V_i - V_0) d'_4[n + 1] T_s}{L_1} \quad (7)$$

Regrouping variables and solving for the predicted duty cycle yields,

$$d_4[n + 1] = \frac{L_1}{(V_{uc} + V_0) T_s} [i(n + 1) - i(n - 1)] + 2 \frac{V_0 - V_i}{V_{uc} + V_0} - d_4[n] \quad (8)$$

3.4. Mode IV

This is another hybrid mode in which secondary storage (V_{uc}) assists primary storage port (V_b) and delivers power to the load port. This mode (Figure 2(d)) is initiated when both the primary source port (V_i) and primary storage port (V_b) are below the threshold level. Inductor charges when switching devices S_1, S_3 and S_4 are ON in state I and discharges to the load when switching devices S_1 and D_2 are ON in state II. The predicted duty cycle for $(n + 1)^{th}$ cycle could be predicted by,

$$d_4[n + 1] = \frac{L_1}{(V_{uc} + V_0) T_s} [i(n + 1) - i(n - 1)] - d_4[n] + 2 \frac{V_0 - V_b}{V_{uc} + V_0} \quad (9)$$

3.5. Mode V

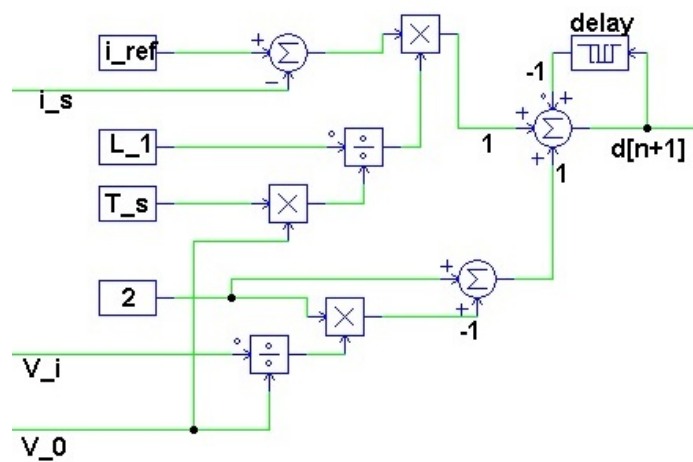
This is an unique mode which transfers power from primary source port (V_i) to primary storage port (V_b). Excess energy produced when the load is off could be stored for future use. The active switching devices are S_3, D_1 and D_3 are during the state I and S_2 and D_1 during state II (refer Figure 3(a)). The value for the predicted duty cycle could be computed using,

$$d_4[n + 1] = 2 - d_4[n] + \frac{L_1}{V_b T_s} [i(n + 1) - i(n - 1)] + 2 \frac{V_i}{V_b} \quad (10)$$

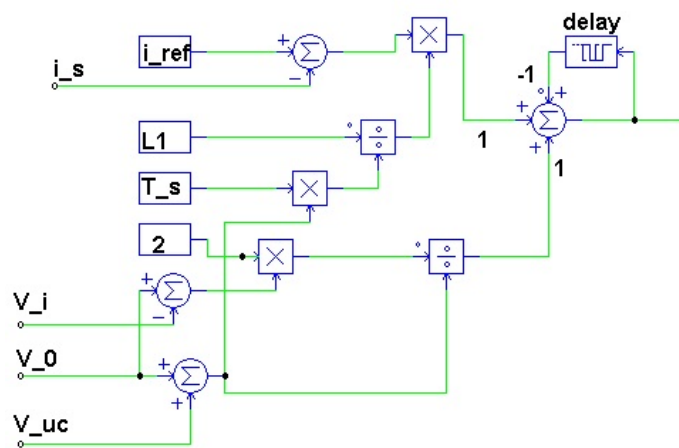
3.6. Mode VI

This mode facilitates reverse power flow. The regenerated energy from the load port is fed back to the secondary storage port V_{uc} . This mode replicates the operation of a buck-boost converter as it provides voltage reduction and inversion. The first switching state in this mode as in (Figure 3(b)) shows the switches S_5 is ON. During the second switching state, energy stored in inductor L_2 will be transferred to the secondary storage port. The duty cycle prediction could be done using the following relation,

$$d_5[n + 1] = \frac{L_2}{(V_0 - V_{uc})T_s} [i(n + 1) - i(n - 1)] - d_5[n] - 2 \frac{V_{uc}}{V_0 - V_{uc}} \tag{11}$$



(a) Mode I

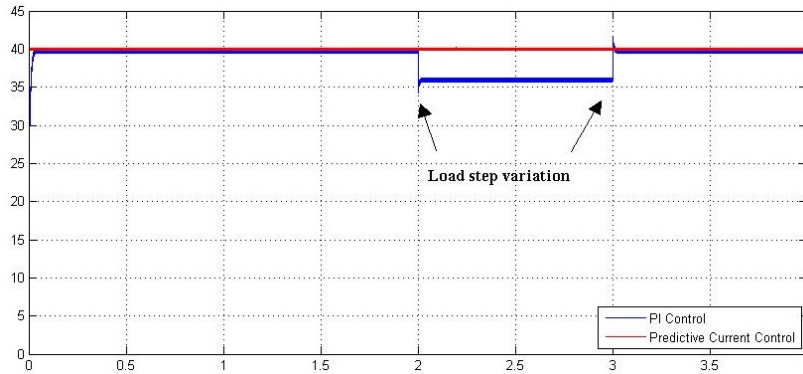


(b) Mode III

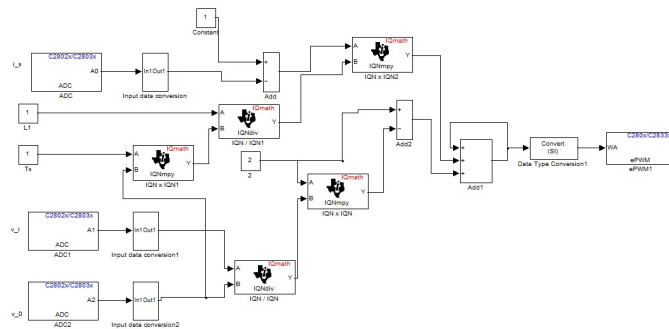
Figure 5. Controller Structure

4. PREDICTIVE CURRENT CONTROLLER LAWS

This section describes the controller for the Four Port Converter. This converter has different operating modes. The control objective is to regulate the inductor current based on a fixed reference value. So the converter requires two controllers: one for mode selection and other for inductor current control. An MATLAB based Stateflow controller is used to select a particular mode based on the measured system parameters. While this work focuses on the utilization of predictive current control for FPC, the Stateflow controller is discussed in [8]. Control laws for different operating modes are derived out in the previous section. By making the inductor current $i(n + 1)$ in the $(n + 1)^{th}$ switching cycle equal to the reference current i_{ref} , the inductor current could be made to follow the reference exactly.



(a) Inductor current with PI Controller and Predictive Current controller



(b) Simulink Model for Code Generation

Figure 6. Dynamic waveform and related simulink control model

By substituting,

$$\begin{aligned} i(n + 1) &= i_{ref} \\ i(n - 1) &= i_s \end{aligned} \tag{12}$$

where i_s is the sampled current. By substituting Eq.12 in final equation corresponding to Mode I (Eq.4), it becomes

$$d_3[n + 1] = 2 - d_3[n] + \frac{L_1}{V_0 T_s} [i_{ref} - i_s] - 2 \frac{V_i}{V_0} (Mode I) \tag{13}$$

Doing the similar substitutions in Eqns.6,8,9,10&11, the final equations for duty cycle computation becomes,

$$d_3[n + 1] = 2 - d_3[n] + \frac{L_1}{V_0 T_s} [i_{ref} - i_s] - \frac{2V_b}{V_0} (Mode II) \tag{14}$$

$$d_4[n + 1] = \frac{L_1}{(V_{uc} + V_0) T_s} [i_{ref} - i_s] - d_4[n] + 2 \frac{V_0 - V_i}{V_{uc} + V_0} (Mode III) \tag{15}$$

$$d_4[n + 1] = \frac{L_1}{(V_{uc} + V_0) T_s} [i_{ref} - i_s] - d_4[n] + 2 \frac{V_0 - V_b}{V_{uc} + V_0} (Mode IV) \tag{16}$$

$$d_4[n + 1] = 2 - d_4[n] + \frac{L_1}{V_b T_s} [i_{ref} - i_s] + 2 \frac{V_i}{V_b} (Mode V) \tag{17}$$

$$d_5[n + 1] = \frac{L_2}{(V_0 - V_{uc}) T_s} [i_{ref} - i_s] - d_5[n] - 2 \frac{V_{uc}}{V_0 - V_{uc}} (Mode VI) \tag{18}$$

The proposed predictive current controller for FPC is simulated using PSIM. The measured parameters are communicated to the Stateflow controller through an Outlink node. As described before, a Stateflow controller decides the operating mode and communicate to PSIM through an Inlink node. Based on the command received, a specific operating mode is activated and the corresponding current control is activated. A schematic diagram of Mode I is shown in Figure 5a. The final equations of Mode I, II and V(Eq.13,14,17) has a similar structure and could be implemented just by switching variables used for the computation of the predicted duty cycle. In the same way, Mode III(Figure 5b) and IV has a similar structure so that these could use the same building block.

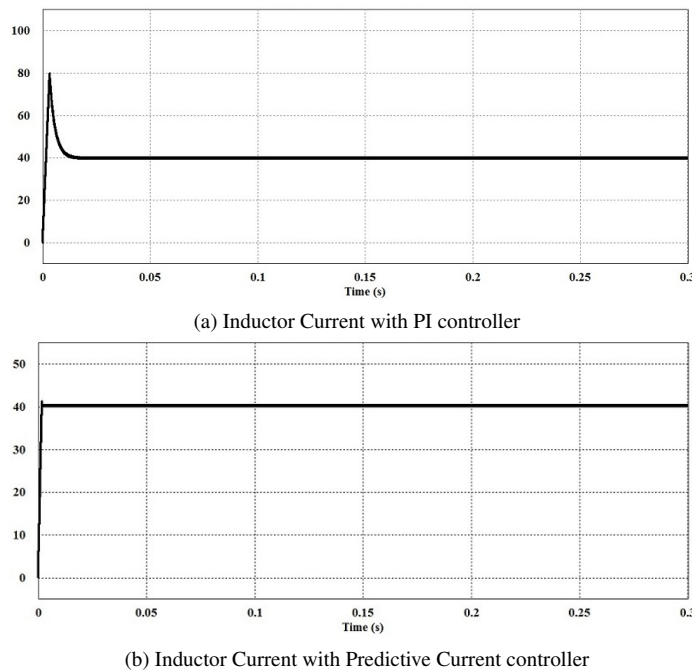


Figure 7. Steady state waveforms

5. RESULT AND ANALYSIS

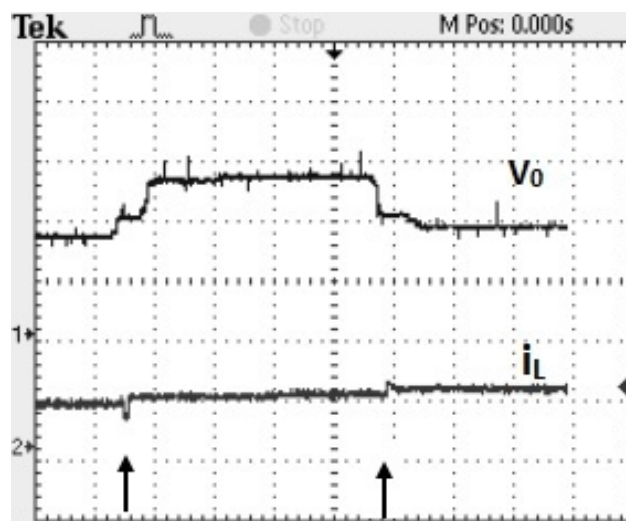
This section presents the steady-state and dynamic results of the proposed predictive current control methodology. Simulation is done using the co-simulation tool of PSIM utilizing MATLAB. Simulation results of Mode I using PI controller and the proposed Predictive Current Controller in steady state is shown in Figure 7. The steady-state waveforms show a reduced current ripple in using PCC compared to the PI controller. The controller is subjected to a step variation in load and the results are shown in Figure 6a. The PI controller goes for a spike and settles while the PCC controller results show that the inductor current exactly follows the reference irrespective of a variation in load. The Predictive Current Controller is implemented using a Piccolo DSP controller. The controller is programmed using the Embedded Coder toolbox of MATLAB/Simulink with support from Code Composer Studio V3.3. The Simulink model used for code generation is shown in Figure 6b. For experimental verification, a Photo Voltaic(PV) panel(12V,200Wp) is connected to the primary source port. A 14V, 5Ah battery is deployed in primary storage port and two ultracapacitors each of 2.7V, 50F rating, are connected in series and utilized as the secondary storage unit. A step variation in load is applied to the FPC through mechanical arrangement and its results in PI controller($K_p=0.104117$, $K_i=0.0334486$) is shown in Figure 8a. The response to the step variation in load for PCC is presented in Figure 8b. The Predictive Current Controller responds quickly to a step variation and keeps the inductor current exactly equal to the reference value.

6. CONCLUSION

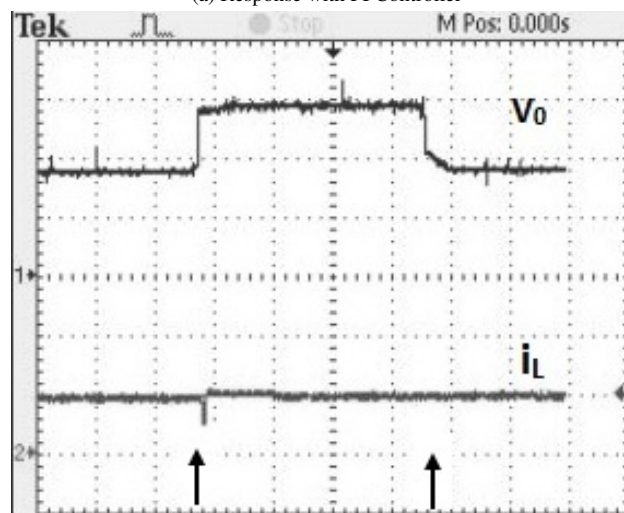
This paper proposes a predictive current control technique for a Four Port DC/DC converter. As the converter has six different operating modes, a Stateflow controller is used for mode selection and PCC is utilized for inductor current control. The control laws to predict the duty cycle for each operating mode is derived out. The feasibility of the proposed control methodology verified using simulation and hardware. The proposed controller provides the advantage of low current ripple and draw constant current from the sources (PV and Battery) which improves the life span of both. The results are compared to a traditional PI controller and show improvements in current ripple minimization, faster dynamic performance and is more suitable for current sensitive Hybrid Electric Vehicle applications.

REFERENCES

- [1] C. Larouci, K. Ejjabraoui, P. Lefranc, and C. Marchand, "Impact of Control Constraint on A Multi-Objective Buck Converter Design," *International Journal of Power Electronics and Drive Systems*, vol. 2, no. 3, pp. 257–266, 2012.



(a) Response with PI Controller



(b) Response with Predictive Current Controller

Figure 8. Dynamic response to step variation in load

- [2] J. Shieh, "Closed-form oriented loop compensator design for peak current-mode controlled DCDC regulators," *IEE Proceedings - Electric Power Applications*, vol. 150, no. 3, p. 351, 2003.
- [3] R. Askour and B. B. Idrissi, "DSP-Based Sensorless Speed Control of a Permanent Magnet Synchronous Motor using Sliding Mode Current Observer," *International Journal of Power Electronics and Drive Systems*, vol. 4, no. 3, pp. 281–289, 2014.
- [4] W. M. Utomo, S. S. Yi, Y. M. Y. Buswig, Z. a. Haron, a. a. Bakar, and M. Z. Ahmad, "Voltage Tracking of a DC-DC Flyback Converter Using Neural Network Control," *International Journal of Power Electronics and Drive Systems*, vol. 2, no. 1, pp. 35–42, 2012.
- [5] A. Kouzou, H. A. Rub, M. O. Mahmoudi, M. S. Boucherit, and R. Kennel, "Current/voltage ripple minimization of DC/DC interface system for renewable energies," in *International Aegean Conference on Electrical Machines and Power Electronics and Electromotion, Joint Conference*. IEEE, Sep. 2011, pp. 758–763.
- [6] S. Changchien, T. Liang, J. Chen, and L. Yang, "Fast Response DC/DC Converter with Transient Suppression Circuit," in *37th IEEE Power Electronics Specialists Conference*. IEEE, 2006, pp. 1–5.
- [7] S. Vesti, J. Oliver, R. Prieto, J. Cobos, and T. Suntio, "Stability and transient performance assessment in a COTS-module-based distributed DC/DC system," in *2011 IEEE 33rd International Telecommunications Energy Conference (INTELEC)*. IEEE, Oct. 2011, pp. 1–7.
- [8] T. K. Santhosh, K. Natarajan, and C. Govindaraju, "Synthesis and Implementation of Multi-Port DC/DC Converter for Hybrid Electric Vehicle," *Journal of Power Electronics*, vol. 15, no. 5, pp. 1178–1189, 2015.

- [9] A. Prodic, R. R. W. Erickson, D. Maksimovic, J. Chen, A. Prodić, R. R. W. Erickson, and D. Maksimović, "Predictive digital current programmed control," *IEEE Transactions on Power Electronics*, vol. 18, no. 1 II, pp. 411–419, Jan. 2003.
- [10] W. Fang, X.-D. Liu, S.-C. Liu, and Y.-F. Liu, "A Digital Parallel Current-Mode Control Algorithm for DCDC Converters," *IEEE Transactions on Industrial Informatics*, vol. 10, no. 4, pp. 2146–2153, Nov. 2014.
- [11] M. Hallworth and S. A. Shirsavar, "Microcontroller-Based Peak Current Mode Control Using Digital Slope Compensation," *IEEE Transactions on Power Electronics*, vol. 27, no. 7, pp. 3340–3351, Jul. 2012.
- [12] Z. Shen, X. Chang, W. Wang, X. Tan, N. Yan, and H. Min, "Predictive Digital Current Control of Single-Inductor Multiple-Output Converters in CCM With Low Cross Regulation," *IEEE Transactions on Power Electronics*, vol. 27, no. 4, pp. 1917–1925, Apr. 2012. [Online]. Available: <http://ieeexplore.ieee.org/lpdocs/epic03/wrapper.htm?arnumber=6020807>

BIOGRAPHY OF AUTHORS



Santhosh T K received his B.E degree in Electrical and Electronics Engineering from Kumaraguru College of Technology, Coimbatore, India in 2009 and M.E degree in Power Electronics and Drives from K.S.R.College of Engineering, Tiruchengode, India in 2011. He is currently working towards Ph.D in Electrical Engineering at Government College of Engineering, Salem under Anna University, Chennai. His research interest includes multiple input converters for electric vehicle, digital control of power electronic systems and renewable energy.



Govindaraju C received his B.E degree in Electrical and Electronics Engineering from Government College of Engineering, Salem, in 1999 and M.E degree in Power Electronics and Drives from College of Engineering, Anna University, Chennai, in 2003. He received Ph.D in the field of energy efficient multilevel inverters from Anna University, Chennai in 2011. He is an Assistant Professor in department of Electrical and Electronics Engineering, Government College of Engineering, Salem, Tamilnadu, India. His research interest includes multilevel inverters, power electronics interface for renewable energy systems, and Smart grids.